PERGAMON

www.elsevier.nl/locate/poly

Polyhedron 19 (2000) 913–923

POLYHEDRON

Palladium(II), platinum(II), and platinum(IV) complexes containing *trans*-1,2-bis(diphenylphosphino)ethene or *cis*,*trans*,*cis*-1,2,3,4-tetrakis(diphenylphosphino)cyclobutane: complete X-ray structural characterization of binuclear compounds

Werner Oberhauser [a], Thomas Stampfl [a], Christian Bachmann [a], Rainer Haid [a], Christoph Langes [a], Holger Kopacka [a], Karl-Hans Ongania [b], Peter Brüggeller [a,*]

[a] *Institut für Allgemeine, Anorganische und Theoretische Chemie, Universität Innsbruck, Innrain 52a, 6020 Innsbruck, Austria*

[b] *Institut für Organische Chemie, Universität Innsbruck, Innrain 52a, 6020 Innsbruck, Austria*

Received 8 December 1999; accepted 11 February 2000

Abstract

Several novel binuclear Pd^{II}, Pt^{II}, and Pt^{IV} complexes of *trans*-1,2-bis(diphenylphosphino)ethene (*trans*-dppen) or *cis*,*trans*,*cis*-1,2,3,4-tetrakis(diphenylphosphino)cyclobutane (dppcb) have been prepared and characterized by X-ray diffraction methods, $^{195}Pt\{^1H\}$ and $^{31}P\{^1H\}$ NMR spectroscopy, FAB mass spectrometry, IR spectroscopy, elemental analyses and melting points. The X-ray structure and NMR parameters of $[Pt_2I_4(trans\text{-dppen})_2]$ (**1**) confirm that homobimetallic complexes of the type $[M_2L_4(trans\text{-dppen})_2]$ ($M = Ni, Pd, Pt$; $L = Cl^-, I^-, CN^-$) contain two square planar coordination units joined by two *trans*-dppen bridges in the solid as well as in the solution state. An analogous structure type is retained in the Pt^{IV} compound $[Pt_2Cl_8(trans\text{-dppen})_2]$ (**2**). In contrast to the corresponding Pt^{II} complex of the new tetradentate phosphine dppcb, the X-ray structure of $[Pd_2Cl_4(dppcb)]$ (**3**) reveals only one conformation. This can be explained by the longer Pd–P bonds compared with the Pt–P bonds and the weaker square planar stabilization energy in **3**. In **3** dppcb acts as a binuclear tetraligate single-bridging ligand combining two square planar coordination centres. The reaction of $Pd(CN)_2$ with dppcb leads to $[Pd_2(CN)_4(dppcb)]$ (**4**). The removal of the coordinated chlorides in **3** by $AgBF_4$ followed by subsequent treatment with $NaNO_2$ produces $[Pd_2(NO_2)_4(dppcb)]$ (**5**). In an analogous reaction with 1,10-phenanthroline (phen) or 2,2′-bipyridine (bipy), $[Pd_2(dppcb)(phen)_2](BF_4)_4$ (**6**) and $[Pd_2(dppcb)(bipy)_2](BF_4)_4$ (**7**) are formed. The complexes **4**–**7** show structure types corresponding to the X-ray structure of **3**. The same is true for the treatment of **3** with $PMePh_2$ or PMe_2Ph, where $[Pd_2(dppcb)(PMePh_2)_4](BF_4)_2Cl_2$ (**8**) and $[Pd_2(dppcb)(PMe_2Ph)_4](BF_4)_4$ (**9**) are obtained. However, the X-ray structure of **8** reveals that the chlorides are coordinated in the solid state, and the crystal structure consists of *trans*-$[Pd_2Cl_2(dppcb)(PMePh_2)_2](BF_4)_2$ (**10**). The flexibility and stereochemical demands of dppcb in the compounds **3**–**10** and related species are discussed in view of the possible application of Pd^{II} complexes containing bidentate tertiary phosphine ligands as catalysts for the alternating copolymerization of ethene and carbon monoxide. In this respect dppcb can be regarded as a combination of two bidentate phosphines, where the cyclobutane ring corresponds to a relatively rigid ligand backbone. This produces strain in the five-membered rings of **3**–**10** which is released by 'envelope'-folding in the X-ray structures of **3** and **10**.

Keywords: Crystal structures; Palladium complexes; Platinum complexes; Diphosphine complexes; Tetraphosphine complexes; Bimetallic complexes

1. Introduction

Trans-1,2-bis(diphenylphosphino)ethene (*trans*-dppen) is a diphosphine-like 1,2-bis(diphenylphosphino)acetylene (dppa), in which the rigidity of the unsaturated carbon backbone forces two phosphorus atoms to remain too far apart for them both to bond to a single metal atom [1–3]. Furthermore, *trans*-dppen bridges preclude the possibility of a bridging halogen atom between the metal centres in bimetallic species, where the number of *trans*-dppen bridges varies from one to four [4–6]. In this work the structure of homobimetallic complexes of the type $[M_2L_4(trans\text{-dppen})_2]$ ($M = Ni, Pd, Pt$; $L = Cl^-, I^-, CN^-$) [7,8] is confirmed by the X-ray structure of the novel compound $[Pt_2I_4(trans\text{-dppen})_2]$ (**1**) corresponding to structure type (a) in Scheme 1. The NMR

* Corresponding author. Tel.: +43-512-507-5115; +43-512-507-2934; e-mail: peter.brueggeller@uibk.ac.at

0277-5387/00/$ - see front matter
PII S0277-5387(00)00332-6

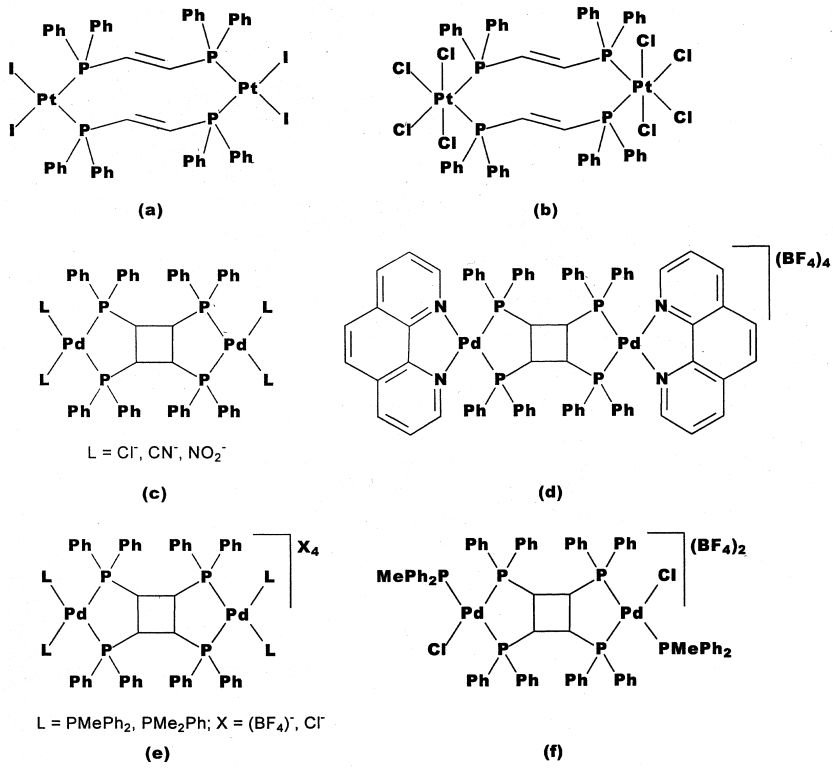

Scheme 1. Structure types observed in compounds **1**–**10**. Structure (a) occurs in $[Pt_2I_4(trans\text{-dppen})_2]$ (**1**), structure (b) in $[Pt_2Cl_8(trans\text{-dppen})_2]$ (**2**), structure (c) in $[Pd_2L_4(dppcb)]$ ($L=Cl^-$ (**3**), $L=CN^-$ (**4**), $L=NO_2^-$ (**5**)), structure (d) in $[Pd_2(dppcb)(phen)_2](BF_4)_4$ (**6**) and analogous to it in $[Pd_2(dppcb)(bipy)_2](BF_4)_4$ (**7**), structure (e) in $[Pd_2(dppcb)(PMePh_2)_4](BF_4)_2Cl_2$ (**8**) and $[Pd_2(dppcb)(PMe_2Ph)_4](BF_4)_4$ (**9**), and structure (f) in *trans*-$[Pd_2Cl_2(dppcb)(PMePh_2)_2](BF_4)_2$ (**10**).

parameters of **1** indicate that the same structure is retained in solution. The Pt^{IV} complex $[Pt_2Cl_8(trans\text{-dppen})_2]$ (**2**) shows the analogous structure type (b) in Scheme 1.

Only recently, *trans*-dppen together with Pt^{II} as a template have been used to produce the new tetradentate phosphine *cis,trans,cis*-1,2,3,4-tetrakis(diphenylphosphino)cyclobutane (dppcb) [7]. Comparable to the tetratertiary phosphine 2,3-bis[(diphenylphosphino)methyl]-1,4-bis(diphenylphosphino)butane, dppcb coordinates in a bis(bidentate) manner to two metals and favours homobimetallic complexes [9]. However, the rigidity of the cyclobutane ring in dppcb prevents the coordination of all four phosphorus atoms to one metal. Pd^{II} complexes containing bidentate tertiary phosphine ligands show high catalyst activity and yield for alternating CO/ethene copolymerization and opened the way for efficient synthesis of polyketone [10], where dppcb can be regarded as a combination of two bidentate phosphines. Since also Pd^{II} complexes of nitrogen-containing bidentate ligands are very active precatalysts in the copolymerization of styrene with carbon monoxide, an investigation of the structural possibilities of bimetallic Pd^{II} complexes with dppcb is interesting [11]. Therefore, the novel compounds $[Pd_2L_4(dppcb)]$ ($L=Cl^-$ (**3**), CN^- (**4**), NO_2^- (**5**)), $[Pd_2(dppcb)(phen)_2](BF_4)_4$ (**6**) and $[Pd_2(dppcb)(bipy)_2](BF_4)_4$ (**7**), where phen and bipy are 1,10-phenanthroline and 2,2′-bipyridine, respectively, have been prepared. They belong to structure types (c) and (d) in Scheme 1, where **7** is analogous to **6**, and have been confirmed by the X-ray structure of **3**.

Furthermore, in order to extend the type of potentially catalytic active compound for oligomerization and polymerization of olefins, Pd^{II} complexes of the type $[PdCl(diphosphine)(monophosphine)]^+$ have been synthesized [12]. The corresponding new complexes containing dppcb $[Pd_2(dppcb)(PMePh_2)_4](BF_4)_2Cl_2$ (**8**), $[Pd_2(dppcb)(PMe_2Ph)_4](BF_4)_4$ (**9**), and *trans*-$[Pd_2Cl_2(dppcb)(PMePh_2)_2](BF_4)_2$ (**10**) show structure types (e) and (f) in Scheme 1. Upon crystallization of **8**, the chloride anions coordinate to Pd^{II} and **10** is formed. **10** is fully characterized by an X-ray structure analysis.

2. Experimental

2.1. Reagents and chemicals

Reagent grade chemicals were used as received unless stated otherwise. *Trans*-1,2-bis(diphenylphosphino)ethene (*trans*-dppen) was purchased from Aldrich. $PMePh_2$ and PMe_2Ph were obtained from Strem. All other reagents and solvents were received from Fluka. Solvents used for NMR measurements and crystallization purposes were of purissimum grade quality. $PdCl_2$ and $Na_2PtCl_4\cdot 4H_2O$ were also obtained from Fluka.

2.2. Instrumentation

Fourier-mode $^{195}Pt\{^1H\}$ and $^{31}P\{^1H\}$ NMR spectra were obtained using Bruker AC-200 and DPX-300 spectrometers (internal deuterium lock) and were recorded at 43.02 (64.50) and 80.96 (121.44) MHz, respectively. Positive chemical shifts are downfield from the standards, where 1.0 M Na_2PtCl_6 and 85% H_3PO_4 were used as standards, respectively.

2.3. Syntheses of Pd^{II}, Pt^{II}, and Pt^{IV} complexes

A Schlenk apparatus and oxygen-free, dry Ar were used in the syntheses of all complexes. Solvents were degassed by several freeze–pump–thaw cycles prior to use. All reactions were carried out at room temperature unless stated otherwise. [Pt_2Cl_4(*trans*-dppen)$_2$] and dppcb were prepared as described earlier [7].

2.3.1. [Pt_2I_4(*trans*-dppen)$_2$] (**1**)

[Pt_2Cl_4(*trans*-dppen)$_2$] (0.075 mmol, 0.100 g) was dissolved in CH_2Cl_2/DMF (v/v = 2:1, 5 cm^3) and LiI (0.30 mmol, 0.040 g) was added with vigorous stirring and prevention of light. The reaction mixture was stirred at 45°C for 48 h. Then the solvent was completely removed, the yellow residue was filtered off in H_2O, washed with H_2O and dried in vacuo. An ochre-yellow powder was recrystallized from CH_2Cl_2/Et_2O. Yield 0.100 g (79%); m.p. > 310°C. *Anal*. Found: C, 36.8; H, 2.7. Calc. for $C_{52}H_{44}I_4P_4Pt_2$: C, 36.9; H, 2.6%. A sample for X-ray diffraction with the composition $C_{52}H_{44}I_4P_4Pt_2 \cdot 0.75$DMF was crystallized from $CHCl_3$/DMF with prevention of light.

2.3.2. [Pt_2Cl_8(*trans*-dppen)$_2$] (**2**)

Chlorine was bubbled through a solution of [Pt_2Cl_4(*trans*-dppen)$_2$] (0.075 mmol, 0.100 g) in DMF (10 cm^3) for 10 min with prevention of light. The volume of the solvent was reduced and a yellow precipitate formed. Then Et_2O was added, the precipitate was filtered off and dried in vacuo. A yellow powder was recrystallized from DMF. Yield 0.079 g (72%); m.p. 192–194°C. *Anal*. Found: C, 42.4; H, 3.1. Calc. for $C_{52}H_{44}Cl_8P_4Pt_2$: C, 42.6; H, 3.0%.

2.3.3. [Pd_2Cl_4(dppcb)] (**3**)

$PdCl_2$ (0.50 mmol, 0.089 g) was suspended in DMF (7 cm^3). Then dppcb (0.25 mmol, 0.198 g) was added with vigorous stirring. The reaction mixture was stirred at 55°C for 6 h and a white precipitate formed. The solvent was completely removed, the white residue was filtered off in CH_2Cl_2, washed with CH_2Cl_2 and dried in vacuo. A white powder was recrystallized from DMF. Yield 0.328 g (91%); m.p. > 320°C. *Anal*. Found: C, 53.2; H, 5.1; N, 3.8. Calc. for $C_{52}H_{44}Cl_4P_4Pd_2 \cdot 4$DMF: C, 53.4; H, 5.0; N, 3.9%. A sample for X-ray diffraction with the composition $C_{52}H_{44}Cl_4P_4Pd_2 \cdot 4$DMF was crystallized from DMF.

2.3.4. [$Pd_2(CN)_4$(dppcb)] (**4**)

Compound **4** was prepared in an analogous manner to **3**, where $Pd(CN)_2$ (0.50 mmol, 0.079 g) was used. A white powder was recrystallized from DMF. Yield 0.227 g (82%); m.p. 304°C. IR (KBr, cm^{-1}) CN: 2135 ν. *Anal*. Found: C, 60.4; H, 4.2; N, 4.8. Calc. for $C_{56}H_{44}N_4P_4Pd_2$: C, 60.6; H, 4.0; N, 5.0%.

2.3.5. [$Pd_2(NO_2)_4$(dppcb)] (**5**)

Compound **3** (0.060 mmol, 0.069 g) was suspended in DMF (6 cm^3). Then $AgBF_4$ (0.24 mmol, 0.047 g) was added with stirring. The reaction mixture was stirred for 2 h, the formed AgCl was filtered off and the solvent completely removed. The residue was dissolved in CH_2Cl_2/DMF (v/v = 10:1, 5 cm^3) and $NaNO_2$ (0.24 mmol, 0.017 g) was added slowly with vigorous stirring. After 5 h the solvent was completely removed, the yellowish residue was filtered off in H_2O, washed with H_2O and dried in vacuo. A yellowish powder was recrystallized from DMF. Yield 0.060 g (84%); m.p. 270–272°C dec. IR (KBr, cm^{-1}) NO_2: 1370 ν_a, 1318 ν_s, 814 δ. *Anal*. Found: C, 52.4; H, 3.7; N, 4.5. Calc. for $C_{52}H_{44}N_4O_8P_4Pd_2$: C, 52.5; H, 3.7; N, 4.7%.

2.3.6. [Pd_2(dppcb)(phen)$_2$](BF_4)$_4$ (**6**)

Compound **3** (0.060 mmol, 0.069 g) was suspended in DMF (6 cm^3). Then $AgBF_4$ (0.24 mmol, 0.047 g) was added with stirring. The reaction mixture was stirred for 2 h, the formed AgCl was filtered off and the solvent completely removed. The residue was dissolved in CH_2Cl_2 (5 cm^3) and 1,10-phenanthroline · H_2O (0.12 mmol, 0.024 g) was added slowly with vigorous stirring. A white precipitate immediately formed. After 5 h the precipitate was filtered off, washed with CH_2Cl_2 and dried in vacuo. A white powder was recrystallized from DMF. Yield 0.084 g (82%); m.p. > 320°C. *Anal*. Found: C, 53.3; H, 3.8; N, 3.2. Calc. for $C_{76}H_{60}B_4F_{16}N_4P_4Pd_2$: C, 53.3; H, 3.5; N, 3.3%.

2.3.7. [Pd_2(dppcb)(bipy)$_2$](BF_4)$_4$ (**7**)

Compound **7** was prepared in an analogous manner to **6**, where 2,2′-bipyridine (0.12 mmol, 0.019 g) was used. A white powder was recrystallized from DMF. Yield 0.062 g (62%); m.p. > 320°C. *Anal*. Found: C, 51.7; H, 3.7; N, 3.3. Calc. for $C_{72}H_{60}B_4F_{16}N_4P_4Pd_2$: C, 51.9; H, 3.6; N, 3.4%.

2.3.8. [Pd_2(dppcb)($PMePh_2$)$_4$](BF_4)$_2Cl_2$ (**8**) and trans-[Pd_2Cl_2(dppcb)($PMePh_2$)$_2$](BF_4)$_2$ (**10**)

Compound **3** (0.090 mmol, 0.104 g) was suspended in CH_2Cl_2/DMF (v/v = 7:1, 10 cm^3). Then $AgBF_4$ (0.18 mmol, 0.035 g) was added with stirring. The reaction mixture was stirred for 8 h, the formed AgCl was filtered off and the solvent completely removed. The residue was dissolved in CH_2Cl_2 (8 cm^3) and $PMePh_2$ (0.36 mmol, 0.072 g) was added via a syringe with vigorous stirring. The solution was stirred for 5 h. The ^{31}P ^1H NMR parameters of this solution correspond to **8**. The solvent was completely removed, the yellow residue was filtered off in EtOH, washed with EtOH

and dried in vacuo. A yellow powder was recrystallized from CH_2Cl_2. Yield 0.120 g (73%); m.p. 220–221°C. FAB mass spectrum: *m/z* 1528.3 $[Pd_2Cl(dppcb)(PMePh_2)_2](BF_4)^+$, 1127.9 $[Pd_2Cl(dppcb)](BF_4)^+$. *Anal.* Found: C, 52.6; H, 4.2. Calc. for $C_{78}H_{70}B_2Cl_2F_8P_6Pd_2 \cdot 2CH_2Cl_2$ corresponding to **10**$\cdot 2CH_2Cl_2$: C, 52.8; H, 4.1%. A sample for X-ray diffraction with the composition $C_{78}H_{70}B_2Cl_2F_8P_6Pd_2 \cdot 2CH_2Cl_2$ was crystallized from CH_2Cl_2.

*2.3.9. $[Pd_2(dppcb)(PMe_2Ph)_4](BF_4)_4$ (**9**)*

Compound **3** (0.060 mmol, 0.069 g) was suspended in DMF (6 cm^3). Then $AgBF_4$ (0.24 mmol, 0.047 g) was added with stirring. The reaction mixture was stirred for 2 h, the formed AgCl was filtered off and the solvent completely removed. The residue was dissolved in CH_2Cl_2/DMF (v/v = 5:1, 5 cm^3) and PMe_2Ph (0.24 mmol, 0.033 g) was added via a syringe with vigorous stirring. After 10 min a yellowish precipitate slowly formed. The slurry was stirred for 5 h. The solvent was completely removed, the yellow residue was filtered off in CH_2Cl_2, washed with CH_2Cl_2 and dried in vacuo. A yellow powder was recrystallized from DMF. Yield 0.053 g (46%); m.p. 208–210°C. FAB mass spectrum: *m/z* 1818.6 $[Pd_2(dppcb)(PMe_2Ph)_4](BF_4)_3^+$, 1593.7 $[Pd_2(dppcb)(PMe_2Ph)_3](BF_4)_2^+$. *Anal.* Found: C, 52.8; H, 4.8. Calc. for $C_{84}H_{88}B_4F_{16}P_8Pd_2$: C, 53.0; H, 4.7%.

2.4. X-ray data collection, structure determination and refinement

Details of the crystal and data collection are summarized in Table 1. The empirical absorption corrections were based on ψ-scans of nine reflections, respectively ($\chi = 78$–$102°$, 360° scans in 10° steps in ψ) [13]. All structure determination calculations were carried out using SHELXTL NT 5.10 including SHELXS-97 [14] and SHELXL-97 [15]. Final refinement on F^2 was carried out with anisotropic thermal parameters for all non-hydrogen atoms. The hydrogen atoms were included using a riding model with isotropic *U* values depending on U_{eq} of the adjacent carbon atoms.

3. Results

*3.1. Crystal structure of $[Pt_2I_4(trans\text{-}dppen)_2]$ (**1**)*

In order to characterize definitely $[Pt_2I_4(trans\text{-}dppen)_2]$ (**1**), its solid state structure was determined by X-ray crystallography. It is a further novel example showing that homobimetallic complexes of *trans*-dppen with d^8 metals are of the type $[M_2L_4(trans\text{-}dppen)_2]$ (M = Ni, Pd, Pt; L = Cl^-, I^-, CN^-) [7,8] corresponding to structure type (a) in Scheme 1. The crystal structure of **1** contains one discrete $[Pt_2I_4(trans\text{-}dppen)_2]$ molecule and a DMF molecule with a site occupation factor of 0.75 per asymmetric unit. Views of **1** are given in Fig. 1; Table 2 contains selected bond distances and bond angles of **1**.

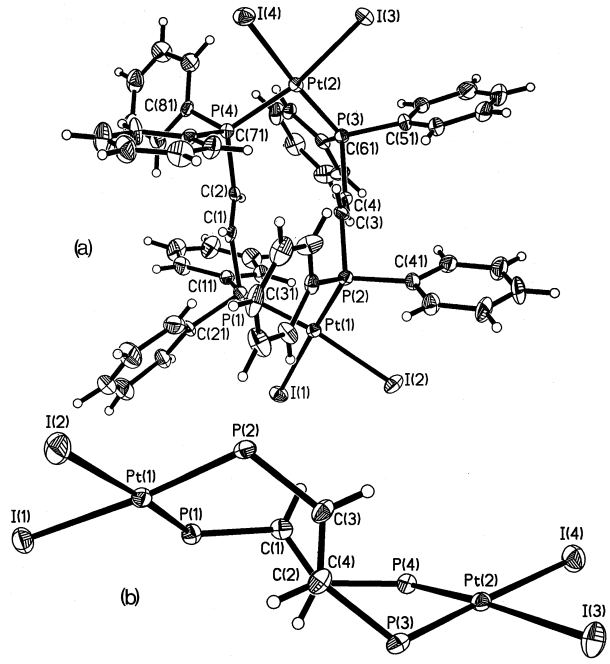

Fig. 1. (a) View of $[Pt_2I_4(trans\text{-}dppen)_2]$ (**1**), showing the atom labelling scheme; (b) C(2)···C(4) projection of $[Pt_2I_4(trans\text{-}dppen)_2]$ (**1**). Phenyl rings omitted for clarity.

The square planar coordinations in **1** are distorted, where the deviations from least-squares planes through the two coordination units are very different: Pt(1) −0.056, I(1) 0.032, I(2) −0.007, P(1) −0.007, P(2) 0.037 Å; Pt(2) −0.070, I(3) 0.109, I(4) −0.082, P(3) −0.079, P(4) 0.121 Å. This is in contrast to $[Pt_2Cl_4(trans\text{-}dppen)_2]$ (**11**) showing a largest deviation of only 0.059 Å for Pt(2) [7]. The difference can be explained by the stronger *trans* influence of I^- versus Cl^- [16,17], producing a longer mean Pt–P bond length of 2.273(5) Å in **1** than of 2.248(3) Å in **11**. Like in the case of other polyphosphines [18], the steric demands of two bridging *trans*-dppen ligands in a *cis* position (see Fig. 1(a)) lead to a 'steric pressure', which is opposed by the electronic demands of Pt(II). The weaker Pt–P bonds in **1** compared with **11** allow a release of the steric strain by larger deviations from ideal square planar coordinations in **1** than in **11**.

Owing to these differences, the angle between the coordination planes of 43.1° in **1** is larger than the corresponding parameter of 39.7° in **11**. This produces a significantly smaller Pt···Pt separation of 6.757(1) Å in **1** compared with 6.800(1) Å in **11**. The P–Pt–P angles of 96.15(11) and 96.65(10)° in **1** are significantly larger than the P–Pt–P angles of 94.77(14) and 95.08(14)° in **11**. This is a further consequence of the weaker Pt–P bonds in **1** than in **11**. This opening of the P–Pt–P angles in **1** leads to longer C(1)···C(3) and C(2)···C(4) distances of 3.093 and 3.076 Å, respectively, compared with the corresponding values of 2.837 and 2.858 Å in **11**. The C(2)···C(4) projection angle between the aliphatic double bonds (Fig. 1(b)) of 37.3° in **1** is very similar to the corresponding value of 37.6° in

Table 1
Crystallographic data for $[Pt_2I_4(trans\text{-dppen})_2]$ (**1**), $[Pd_2Cl_4(dppcb)]$ (**3**), and *trans*-$[Pd_2Cl_2(dppcb)(PMePh_2)_2](BF_4)_2$ (**10**)

	1	**3**	**10**
Empirical formula	$C_{52}H_{44}I_4P_4Pt_2 \cdot 0.75DMF$	$C_{52}H_{44}Cl_4P_4Pd_2 \cdot 4DMF$	$[C_{78}H_{70}Cl_2P_6Pd_2](BF_4)_2 \cdot 2CH_2Cl_2$
Colour	yellow–orange	colourless	colourless
Habit	prismatic	prismatic	irregular
Crystal size (mm)	0.4×0.1×0.1	0.35×0.3×0.1	1.2×0.4×0.2
a (Å)	11.701(2)	14.002(3)	13.484(2)
b (Å)	14.632(3)	13.921(3)	12.592(2)
c (Å)	18.962(4)	16.943(3)	24.452(5)
α (°)	91.53(3)		
β (°)	107.13(3)	105.72(3)	103.80(1)
γ (°)	111.57(3)		
V (Å^3)	2851.7(10)	3179.0(11)	4031.9(12)
Diffractometer	Siemens P4 (Mo Kα radiation)		
Crystal system	triclinic	monoclinic	monoclinic
Space group	$P\bar{1}$	$P2_1/n$	$P2_1/c$
Z	2	2	2
Scan type	ω	ω	ω
No. reflections collected	16142	8527	11222
No. independent reflections	13932	7052	9288
No. observed reflections ($I>3\sigma(I)$)	5210	3106	5579
R_{int}	0.024	0.021	0.029
Completeness (%)	83.7 (θ=1.98–30.00°)	96.6 (θ=2.10–27.49°)	91.0 (θ=2.02–28.50°)
Index ranges	$-1\le h\le 14$, $-20\le k\le 19$, $-26\le l\le 25$	$-1\le h\le 18$, $-1\le k\le 18$, $-21\le l\le 21$	$-1\le h\le 18$, $-1\le k\le 16$, $-31\le l\le 32$
No. parameters	604	374	470
GOF on F^2	0.99	1.02	1.03
Final R indices (observed data)			
R_1 [a]	0.0418	0.0387	0.0428
wR_2 [b]	0.1132	0.1202	0.1149
Largest difference peak (e Å^{-3})	1.45	0.69	1.03
Transmission	0.602–1.000	0.630–0.971	0.650–1.000
T (K)	213	173	213

[a] $R_1=(\sum||F_o|-|F_c||)/\sum|F_o|$.
[b] $wR_2=[(\sum w(F_o^2-F_c^2)^2)/\sum w(F_c^2)^2]^{1/2}$ with weight $=1/[\sigma^2(F_o^2)+(xP)^2+yP]$; $x=0.0414$, $y=0$ for **1**; $x=0.0497$, $y=3.50$ for **3**; $x=0.0564$, $y=10.25$ for **10**; $P=(F_o^2+2F_c^2)/3$.

$[Pd_2Cl_4(trans\text{-dppen})_2]$ [7], but different from the value of 34.8° in **11**. Comparable differences in the orientations of diphosphine-bridges have been observed in the X-ray structures of a series of dimers containing dppa [1–3]. All Pt–I bond lengths in **1** (see Table 2) are located within the typical range also found in $[Pt_2I_4(dppa)_2]$ [2]. Owing to the large P–Pt–P angles in **1**, the I–Pt–I angles of 87.62(5) and 85.81(4)° are significantly reduced to values below 90°, where the same effect is present in $[Pt_2I_4(dppa)_2]$. The X-ray structure of **1** reveals that replacement of Cl^- in **11** by I^- in **1** leads to a fine tuning of the actual structure also with respect to the orientations of the aliphatic double bonds. Since the intramolecular [2+2] photocycloaddition of these double bonds in **11** produces the new tetradentate phosphine dppcb [7], the observed fine tuning is important for the development of further Pt(II) templates, which will be used for the production of other new ligands.

3.2. Crystal structure of $[Pd_2Cl_4(dppcb)]$ (3)

The two conformations of $[Pt_2Cl_4(dppcb)]$ (**12**) seen in its X-ray structure [7] reveal the amount by which this molecular structure varies in the solution phase as the local solvent field varies with time, if we assume as a first approximation that the forces on the molecule in solution are of the same order as those in the solid [19]. Since this flexibility could influence the catalytic properties of homobimetallic complexes of dppcb, the solid state structure of **3** was also determined by X-ray crystallography. It confirms that compounds of the type $[Pd_2L_4(dppcb)]$, where L is Cl^-, CN^- or NO_2^- (**3–5**), $[Pd_2(dppcb)(phen)_2](BF_4)_4$ (**6**), and $[Pd_2(dppcb)(bipy)_2](BF_4)_4$ (**7**) correspond to structure types (c) and (d) in Scheme 1. The crystal structure of **3** consists of two discrete $[Pd_2Cl_4(dppcb)]$ molecules and eight molecules of DMF per unit cell. $[Pd_2Cl_4(dppcb)]$ is located on a centre of symmetry. Views of **3** are given in Fig. 2; Table 3 contains selected bond distances and bond angles of **3**.

As in the case of **12**, owing to crystallographic constraints produced by the centre of symmetry, the cyclobutane ring is completely planar in **3**. The mean C–C bond length of 1.557(4) Å in **3** is, within statistical significance, identical with the same parameter of 1.548(7) Å in **12** and within the usual range of 1.545–1.607 Å [20,21]. The 'envelope'-fold-

Table 2
Selected bond lengths (Å) and angles (°) for $[Pt_2I_4(trans\text{-dppen})_2]$ (**1**)

Pt(1)–P(1)	2.282(3)
Pt(1)–P(2)	2.262(3)
Pt(1)–I(1)	2.6649(13)
Pt(1)–I(2)	2.6355(13)
Pt(2)–P(3)	2.280(3)
Pt(2)–P(4)	2.267(3)
Pt(2)–I(3)	2.6253(13)
Pt(2)–I(4)	2.6450(11)
P(1)–C(11)	1.800(12)
P(1)–C(21)	1.814(10)
P(1)–C(1)	1.826(11)
P(2)–C(31)	1.811(11)
P(2)–C(41)	1.828(11)
P(2)–C(3)	1.804(10)
P(3)–C(51)	1.833(11)
P(3)–C(61)	1.813(11)
P(3)–C(4)	1.834(10)
P(4)–C(71)	1.837(11)
P(4)–C(81)	1.835(12)
P(4)–C(2)	1.826(10)
C(1)–C(2)	1.341(13)
C(3)–C(4)	1.289(14)
P(1)–Pt(1)–P(2)	96.15(11)
P(2)–Pt(1)–I(2)	90.37(8)
P(1)–Pt(1)–I(2)	172.98(7)
P(2)–Pt(1)–I(1)	175.30(7)
P(1)–Pt(1)–I(1)	85.68(8)
I(1)–Pt(1)–I(2)	87.62(5)
P(3)–Pt(2)–P(4)	96.65(10)
P(4)–Pt(2)–I(3)	168.63(7)
P(3)–Pt(2)–I(3)	90.64(8)
P(4)–Pt(2)–I(4)	86.97(8)
P(3)–Pt(2)–I(4)	176.37(7)
I(3)–Pt(2)–I(4)	85.81(4)
C(11)–P(1)–C(21)	106.4(6)
C(11)–P(1)–C(1)	100.3(5)
C(21)–P(1)–C(1)	101.2(5)
C(11)–P(1)–Pt(1)	115.1(4)
C(21)–P(1)–Pt(1)	114.0(4)
C(1)–P(1)–Pt(1)	118.0(3)
C(3)–P(2)–C(31)	106.0(6)
C(3)–P(2)–C(41)	100.1(5)
C(31)–P(2)–C(41)	103.7(5)
C(3)–P(2)–Pt(1)	115.2(4)
C(31)–P(2)–Pt(1)	109.8(4)
C(41)–P(2)–Pt(1)	120.6(4)
C(51)–P(3)–C(61)	102.6(6)
C(61)–P(3)–C(4)	104.9(5)
C(51)–P(3)–C(4)	100.6(5)
C(61)–P(3)–Pt(2)	114.6(4)
C(51)–P(3)–Pt(2)	117.7(4)
C(4)–P(3)–Pt(2)	114.6(4)
C(2)–P(4)–C(81)	100.3(5)
C(2)–P(4)–C(71)	103.1(5)
C(71)–P(4)–C(81)	107.2(5)
C(2)–P(4)–Pt(2)	116.7(3)
C(81)–P(4)–Pt(2)	111.1(4)
C(71)–P(4)–Pt(2)	116.8(4)
C(2)–C(1)–P(1)	120.2(8)
C(1)–C(2)–P(4)	124.4(9)
C(4)–C(3)–P(2)	124.7(10)
C(3)–C(4)–P(3)	124.9(9)

ing of 163.1° for the five-membered rings in **3** (see Fig. 2(b)) is in between the corresponding values of 153.1 and 168.3° for conformations A and B of **12**, respectively. This is reflected in the Pd(1)···Pd(1A) separation of 7.246(1) Å in **3** compared with the Pt···Pt separations of 6.952(1) and 7.327(1) Å in A and B. The same is true for the P(1)–Pd(1)–P(2) angle of 86.40(4)°, which is also in between the P–Pt–P chelate angles of 85.19(11)° in A and 89.11(10)° in B. Thus it seems likely that the effects leading to the two conformations in **12** are balanced in the solid state structure of **3**. The occurrence of two conformations in **12** has been explained by a subtle energetic balance between the preference of dppcb to release the strain of the five-membered rings by a larger 'envelope'-folding in A and the preference of Pt(II) for an ideal square planar environment in B [7]. However, the mean Pd–P bond length of 2.2372(8) Å in **3** is significantly larger than the mean Pt–P bond length of 2.222(2) Å in **12**. This reduces the strain of the five-membered rings in **3**. Furthermore, the square planar stabilization energy is smaller in **3** than in **12** [22]. Both differences lead to the occurrence of only one balanced conformation in **3**. This different flexibility in homobimetallic complexes of dppcb could be important for their catalytic application.

As a consequence of the reduced square planar stabilization energy in **3**, the Pd(1) atom deviates 0.082 Å from a least-squares plane through Cl(1), Cl(2), P(1), and P(2) (see Fig. 2(b)). Comparable large deviations of the Pd atoms in square planar complexes of tetradentate phosphines are well

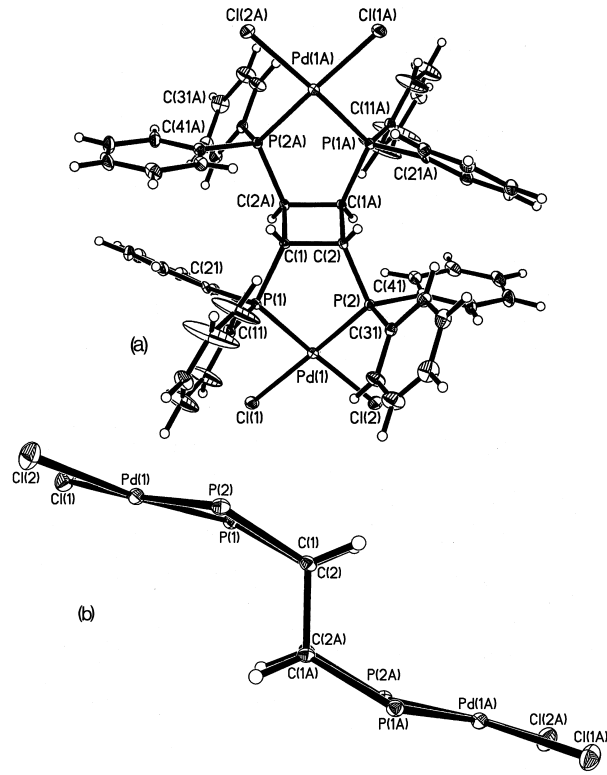

Fig. 2. (a) View of $[Pd_2Cl_4(dppcb)]$ (**3**), showing the atom labelling scheme; (b) view of $[Pd_2Cl_4(dppcb)]$ (**3**) with the cyclobutane plane perpendicular to the projection plane. Phenyl rings omitted for clarity.

Table 3
Selected bond lengths (Å) and angles (°) for $[Pd_2Cl_4(dppcb)]$ (**3**)

Pd(1)–P(1)	2.2402(12)
Pd(1)–P(2)	2.2341(12)
Pd(1)–Cl(1)	2.3638(12)
Pd(1)–Cl(2)	2.3702(13)
P(1)–C(11)	1.815(5)
P(1)–C(21)	1.813(4)
P(1)–C(1)	1.860(4)
P(2)–C(31)	1.829(5)
P(2)–C(41)	1.811(5)
P(2)–C(2)	1.854(4)
C(1)–C(2)	1.558(5)
C(1)–C(2) [a]	1.556(5)
P(1)–Pd(1)–P(2)	86.40(4)
P(1)–Pd(1)–Cl(1)	90.68(5)
P(2)–Pd(1)–Cl(1)	75.29(5)
P(1)–Pd(1)–Cl(2)	173.69(5)
P(2)–Pd(1)–Cl(2)	88.90(5)
Cl(1)–Pd(1)–Cl(2)	93.74(5)
C(11)–P(1)–C(21)	107.4(2)
C(21)–P(1)–C(1)	104.54(19)
C(11)–P(1)–C(1)	105.4(2)
C(21)–P(1)–Pd(1)	117.46(16)
C(11)–P(1)–Pd(1)	111.01(15)
C(1)–P(1)–Pd(1)	110.22(13)
C(31)–P(2)–C(41)	107.3(2)
C(41)–P(2)–C(2)	108.2(2)
C(31)–P(2)–C(2)	102.0(2)
C(41)–P(2)–Pd(1)	116.26(16)
C(31)–P(2)–Pd(1)	111.36(15)
C(2)–P(2)–Pd(1)	110.71(13)
C(2)[a]–C(1)–C(2)	90.4(3)
C(2)[a]–C(1)–P(1)	115.7(3)
C(2)–C(1)–P(1)	114.4(3)
C(1)[a]–C(2)–C(1)	89.6(3)
C(1)[a]–C(2)–P(2)	118.7(3)
C(1)–C(2)–P(2)	113.4(3)

[a] Symmetry transformations used to generate equivalent atoms: $-x+2, -y, -z$.

known and seem to be typical for Pd(II) [9,23]. The Pd–P bond lengths of 2.2402(12) and 2.2341(12) Å in **3** are in the typical range reported previously [9,24] for square planar Pd(II) complexes containing also chelating phosphines *trans* to chlorides. The chelate angle of 86.40(4)° in **3** is comparable to the corresponding parameters of 85.82(3)° in $[Pd(CN)_2$(*cis*-dppen)] [8] and 85.4(1)° in $[Pd(SCN)_2$-(*cis*-dppen)] [25], where *cis*-dppen is *cis*-1,2-bis-(diphenylphosphino)ethene. However, in contrast to **3** and analogous to **12**, $[PdCl_2$(dppe)] shows two conformations with chelate angles of 85.82(7) and 88.3(1)°, where dppe is 1,2-bis(diphenylphosphino)ethane [24,26]. Comparable to $[PdI_2$(*cis*-dppen)]·I_2 [27], in **3** the general impression is that despite the relatively rigid ligand backbone there is little strain in the molecule. The shorter M–P distances in the Pt species **12** are consistent with the stronger Pt–P bonding relative to Pd in **3** [28] and with the 'relativistic or Lanthanide contraction' [8].

3.3. Investigation of *1*–*9* in the solution state

The $^{195}Pt\{^1H\}$ and $^{31}P\{^1H\}$ NMR parameters of compounds **1**–**9** are summarized in Table 4. The NMR data for **1** are consistent with structure (a) in Scheme 1 showing four equivalent phosphorus atoms. This means that the two different diphosphine bridges indicated in the X-ray structure of **1** (see Fig. 1) are equalized in solution at room temperature. The ^1J(Pt,P) value of 3330 Hz in **1** is reduced compared with the analogous parameter of 3550 Hz in **11** in agreement with the stronger *trans* influence of I^- versus Cl^- [16,17] and with the difference of the mean Pt–P bond lengths (see above). The simultaneous presence of this ^1J(Pt,P) value in **1** typical for *trans* iodide and of ^4J(Pt,P) of 41 Hz confirms that complexes of the type $[M_2L_4$(*trans*-dppen)$_2]$ (M = Ni, Pd, Pt; L = Cl^-, I^-, CN^-) [7,8] are also binuclear in solution.

The clean preparation of the Pt(IV) complex **2** by halogenation of the corresponding Pt(II) species **11** indicates that no drastic structural change occurs [29]. This is confirmed by the NMR data for **2**, which are consistent with structure (b) in Scheme 1 also showing four equivalent phosphorus atoms. The δ(Pt) value of −3156 in **2** is comparable with the corresponding parameter of −3226 in the analogous complex $[Pt_2Cl_8(dppa)_2]$ [2]. The same is true for the ^1J(Pt,P) value of 2093 Hz in **2** located in the typical range for a phosphine *trans* to chloride in a Pt(IV) compound [2,16,17]. This is in agreement with *cis* diphosphine bridges, where as in the case of **1** the simultaneous presence of this ^1J(Pt,P) value in **2** typical for *trans* chloride and of ^4J(Pt,P) of 34 Hz confirms the binuclear structure of **2** in solution.

The single $^{31}P\{^1H\}$ NMR resonances for **3**–**7** indicate four equivalent phosphorus atoms in all these compounds, which is consistent with structures (c) and (d) in Scheme 1. The δ(P) downfield shifts of **3**–**7** compared with **1** and **2** show the typical five-ring contribution for chelating dppcb [7,30]. Thus the solution structure of **3** appears to be the same as its solid state structure. In **4** the presence of the cyanides is clearly indicated in the IR spectrum by the C≡N stretching frequency at 2135 cm^{-1}. It is normally found for $[Pd(CN)_2$(monophosphine)$_2]$ complexes that the *cis* isomer is thermodynamically more stable than the *trans* [31], leading to higher C≡N stretching vibrations for cyanides

Table 4
$^{195}Pt\{^1H\}$ and $^{31}P\{^1H\}$ NMR data for **1**–**9** [a]

Compound	δ(Pt)	δ(P)	^1J(Pt,P)	^4J(Pt,P)	^2J(P,P)$_{trans}$
1		1.9	3330	41	
2	−3156t	−6.8	2093	34	
3		78.0			
4		63.2			
5		58.8			
6		85.0			
7		81.0			
8		83.6d			309
		8.4d			309
9		74.0d			307
		10.0d			307

[a] *J* values in Hz. d, doublet; t, triplet. Spectra were run at 298 K. The following solvents were used: CH_2Cl_2 (**1**, **2**, **8**) and DMF (**3**–**7**, **9**).

trans to phosphines [8,32,33] than for cyanides *trans* to cyanides [34]. The stretching value in **4** is in agreement with *cis*-dicyanides. In the case of **5** the direct replacement of the chlorides of **3** by nitrites is not possible, though this transformation has been shown to occur via associative *cis* attack on chloride by nitrite [35]. For **5** the removal of the chlorides from **3** by precipitating AgCl with $AgBF_4$ was necessary for the completion of the reaction with nitrite. The δ(P) value of 77.4 for a DMF solution of the resulting cationic intermediate is consistent with $[Pd_2(dppcb)(DMF)_4](BF_4)_4$, which is analogous to the corresponding Pt(II) complex [7]. The IR spectrum of **5** shows $\nu_a(NO_2)$, $\nu_s(NO_2)$, and δ(ONO) at 1370, 1318, and 814 cm^{-1}, respectively, clearly indicating N-bonded NO_2^- leading to a unidentate nitro complex [36]. This is confirmed by the comparable vibrations in $[PtCl(NO_2)(cis\text{-dppen})]$ [32], where the unidentate N-bonded coordination of NO_2^- has been proven by an X-ray structure analysis [37]. Also for **6** and **7** the removal of the chlorides from **3** by the above procedure was necessary for the completion of the reaction with phen or bipy. The single $^{31}P\{^1H\}$ NMR signals for **6** and **7**, respectively, are consistent with structure (d) in Scheme 1 shown for the phen complex, which is confirmed by the analogous structure found in the corresponding Pt(II) compounds [7]. These complexes are further examples of the tendency for multiple five-ring formation [38].

The reaction of **3** with monophosphines strongly depends on the number of chlorides removed as AgCl. The removal of two chlorides and subsequent treatment with $PMePh_2$ leads to **8**. The $^{31}P\{^1H\}$ NMR data for **8** are in agreement with structure (e) in Scheme 1. The signal with δ(P) of 83.6 is attributed to chelating dppcb showing the typical downfield five-ring contribution [7,30] and the signal with δ(P) of 8.4 to coordinated $PMePh_2$. The $^2J(P,P)_{trans}$ value of 309 Hz is located within the typical range [8,16,23]. However, after isolation of **8** the FAB mass spectrum indicates a strong peak at *m/z* of 1528.3 consistent with $[Pd_2Cl(dppcb)(PMePh_2)_2](BF_4)^+$ and its elemental analysis is in agreement with the loss of two coordinated $PMePh_2$ groups. Since the removal of all chlorides from **3** and subsequent treatment with $PMePh_2$ led to no pure product, the solid state structure of **10** has been clarified by an X-ray structure analysis (see below). In the case of PMe_2Ph the complete replacement of the chlorides in **3** by this monophosphine leading to **9** has been successful. The $^{31}P\{^1H\}$ NMR data for **9** are consistent with structure (e) in Scheme 1. The downfield shifted signal with δ(P) of 74.0 is again attributed to chelating dppcb [7,30] and the signal with δ(P) of -10.0 to coordinated PMe_2Ph. The $^2J(P,P)_{trans}$ value of 307 Hz is nearly identical with the corresponding parameter in **8** and is also located within the typical range [8,16,23]. After isolation of **9** the FAB mass spectrum and elemental analysis are in full agreement with its formulation as $[Pd_2(dppcb)(PMe_2Ph)_4](BF_4)_4$.

The ^1H NMR resonances (CH_2Cl_2-d^2) for the aromatic protons in **1**–**9** occur at 6.5–8.2. In **1** and **2** the ^1H NMR signals of the ethene bridges are obscured by these aromatic resonances. For **3**–**9** broad ^1H NMR signals of the cyclobutane protons are observed at 4.2–4.6. In **8** and **9** the methyl group resonances of coordinated $PMePh_2$ and PMe_2Ph, respectively, occur at 2.1. For **3**–**9** the integrated intensities are in agreement with the proposed structures.

3.4. Crystal structure of trans-$[Pd_2Cl_2(dppcb)(PMePh_2)_2](BF_4)_2$ (10)

In order to characterize definitely the product obtained after isolation of **8**, its solid state structure was determined by an X-ray structure analysis. It shows that this product consists of *trans*-$[Pd_2Cl_2(dppcb)(PMePh_2)_2](BF_4)_2$ (**10**) corresponding to structure type (f) in Scheme 1. The crystal structure of **10** consists of two discrete *trans*-$[Pd_2Cl_2(dppcb)(PMePh_2)_2]^{2+}$ cations, four $(BF_4)^-$ anions, and four molecules of CH_2Cl_2 per unit cell. *Trans*-$[Pd_2Cl_2(dppcb)(PMePh_2)_2]^{2+}$ is located on a centre of symmetry. Views of the cation of **10** are given in Fig. 3; Table 5 contains selected bond distances and bond angles of **10**.

As in the cases of **3** and **12**, owing to crystallographic constraints produced by the centre of symmetry, the cyclobutane ring is completely planar in **10**. The mean C–C bond length of 1.556(3) Å in **10** is, within statistical significance, identical with the same parameters in **3** and **12** (see above)

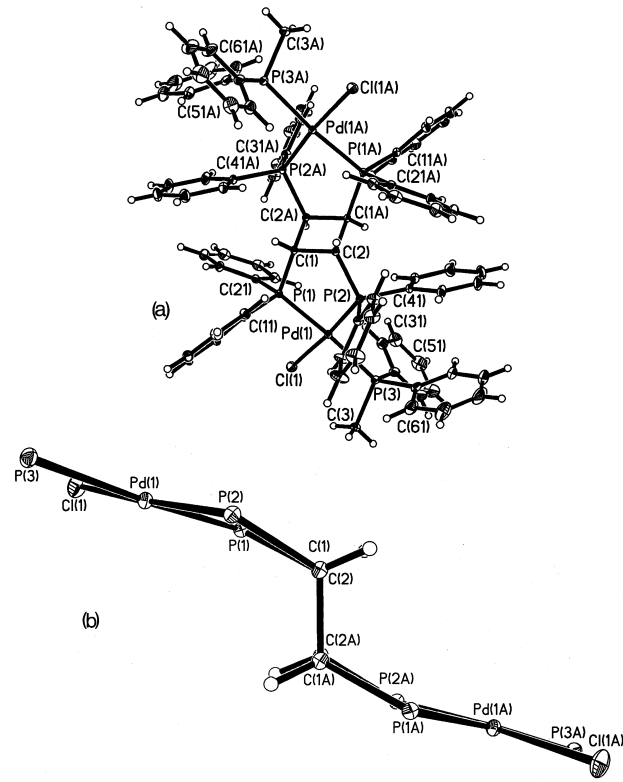

Fig. 3. (a) View of the cation of *trans*-$[Pd_2Cl_2(dppcb)(PMePh_2)_2](BF_4)_2$ (**10**), showing the atom labelling scheme; (b) view of the cation of *trans*-$[Pd_2Cl_2(dppcb)(PMePh_2)_2](BF_4)_2$ (**10**) with the cyclobutane plane perpendicular to the projection plane. Phenyl rings and methyl groups omitted for clarity.

Table 5
Selected bond lengths (Å) and angles (°) for *trans*-[Pd_2Cl_2(dppcb)($PMePh_2$)$_2$](BF_4)$_2$ (**10**)

Pd(1)–P(1)	2.2978(8)
Pd(1)–P(2)	2.2589(8)
Pd(1)–P(3)	2.3753(9)
Pd(1)–Cl(1)	2.3476(8)
P(1)–C(11)	1.810(3)
P(1)–C(21)	1.807(3)
P(1)–C(1)	1.855(3)
P(2)–C(31)	1.815(3)
P(2)–C(41)	1.821(3)
P(2)–C(2)	1.869(3)
P(3)–C(51)	1.813(4)
P(3)–C(61)	1.818(4)
P(3)–C(3)	1.820(3)
C(1)–C(2)	1.559(4)
C(1)–C(2) [a]	1.552(4)
P(1)–Pd(1)–P(2)	85.94(3)
P(1)–Pd(1)–Cl(1)	88.33(3)
P(2)–Pd(1)–Cl(1)	173.76(3)
P(1)–Pd(1)–P(3)	175.22(3)
P(2)–Pd(1)–P(3)	97.77(3)
Cl(1)–Pd(1)–P(3)	87.82(3)
C(11)–P(1)–C(21)	107.07(14)
C(11)–P(1)–C(1)	105.66(14)
C(21)–P(1)–C(1)	106.61(13)
C(11)–P(1)–Pd(1)	108.53(10)
C(21)–P(1)–Pd(1)	117.58(11)
C(1)–P(1)–Pd(1)	110.71(9)
C(31)–P(2)–C(41)	109.63(15)
C(31)–P(2)–C(2)	102.23(14)
C(41)–P(2)–C(2)	106.48(13)
C(31)–P(2)–Pd(1)	112.32(11)
C(41)–P(2)–Pd(1)	114.45(11)
C(2)–P(2)–Pd(1)	110.89(9)
C(51)–P(3)–C(61)	105.92(18)
C(51)–P(3)–C(3)	104.49(18)
C(61)–P(3)–C(3)	102.41(18)
C(51)–P(3)–Pd(1)	110.36(12)
C(61)–P(3)–Pd(1)	121.40(12)
C(3)–P(3)–Pd(1)	110.77(12)
C(2)[a]–C(1)–C(2)	89.5(2)
C(2)[a]–C(1)–P(1)	115.4(2)
C(2)–C(1)–P(1)	114.59(19)
C(1)[a]–C(2)–C(1)	90.5(2)
C(1)[a]–C(2)–P(2)	119.0(2)
C(1)–C(2)–P(2)	114.42(19)

[a] Symmetry transformations used to generate equivalent atoms: $-x+1, -y, -z$.

and also within the usual range [20,21]. However, the smaller 'envelope'-folding of 165.7° for the five-membered rings in **10** (see Fig. 3(b)) compared with the same parameter of 163.1° in **3**, already indicates strain in **10**. Though this produces a significantly larger Pd(1)···Pd(1A) separation of 7.378(1) Å in **10** than of 7.246(1) Å in **3**, the alignment of the phenyl rings containing C(61), C(41), and C(21A) in **10** (see Fig. 3(a)) is necessary to overcome unfavourable repulsive interactions. This stacking of aromatic rings has been observed in complexes of nucleobases also mediated by Pd(II) [39]. The *cis* isomer of **10** is destabilized by these interactions, since one side of the molecule becomes too crowded. A comparable preference of the *trans* isomer has been found for *trans*-[$PdCl(\mu\text{-}PPh_2)(PPh_2H)]_2$ [40]. Also the significantly smaller P(1)–Pd(1)–P(2) chelate angle of 85.94(3)° in **10** compared with 86.40(4)° in **3** is indicative of strain, presumably due to the 'steric pressure' [18] produced by the alignment of the phenyl rings.

The Pd(1)–P(1) bond length of 2.2978(8) Å is significantly larger than the Pd(1)–P(2) bond length of 2.2589(8) Å in **10**, in agreement with the stronger *trans* influence of a phosphine versus chloride [28,41,42]. This difference of Pd–P bond lengths is comparable with the corresponding parameters of 2.284(1) and 2.244(1) Å in [$PdCl(Ph_2PNPPh_2)(PEt_3)$] [12]. The same is true for the Pd–monophosphine bond lengths of 2.3753(9) Å in **10** and 2.366(1) Å in [$PdCl(Ph_2PNPPh_2)(PEt_3)$]. Like in **3** and typical for Pd(II) [9,23], the Pd(1) atom deviates 0.056 Å from a least-squares plane through Cl(1), P(1), P(2), and P(3) (see Fig. 3(b)). There is considerable steric blocking on one side of each coordination unit by the cyclobutane ring and the phenyl groups in **10** (see Fig. 3(a)). This causes an incoming fifth ligand to attach on the other side of the square plane leading to a square pyramidal coordination [43]. Together with the observed steric crowding in **10** leading to the alignment of the phenyl rings, this could initiate the loss of two $PMePh_2$ groups from **8** producing **10**.

When the crystals of **10** are redissolved in CH_2Cl_2/DMF (v/v = 1:1), the $^{31}P\{^1H\}$ NMR spectrum shows three different resonances consistent with the solid state structure of **10**. The single resonance at 81.1, showing the typical downfield five-ring contribution, is attributed to the phopshorus of dppcb *trans* to chloride. Furthermore, two doublets occur at 82.5 (dppcb) and 12.2 ($PMePh_2$), where $^2J(P,P)_{trans}$ is 430 Hz. However, several other signals are also observed in this spectrum indicating that **10** is not stable in solution.

4. Discussion

As already mentioned, some of the new complexes presented in this paper are potentially catalytic active compounds for the alternating CO/ethene copolymerization [10]. In this respect the rigidity of the cyclobutane backbone in homobimetallic complexes of dppcb with Pd(II) together with the orientations of the phenyl rings could influence the activity of these catalysts. Indeed preliminary experiments show that dppcb has beneficial effects on the copolymerization rate [44]. Obviously, like the tripodal the dppcb polyphosphine-control element is so effective that the combined bulk of the ligand–metal assembly and substrate operates to exclude alternatives so that one reaction path is specifically favoured [45]. However, the nature of the metal centre must be finely tuned, depending on the type of reaction involved.

In the case of Rh(I) the binuclear tetraligate single-bridging coordination of dppcb [46] leads to 'mechanical coupling' [47], where preliminary X-ray results show that steric interactions of the phenyl rings comparable with **10** produce

different coordination sites. For the tetradentate phosphine 1,2,4,5-tetrakis(diphenylphosphino)benzene, which is comparable with dppcb, any intramolecular electron transfer in the excited states of its dimetallic complexes also containing Pd(II) relies less on the presence of a low-lying, empty σ* orbital in the ligand than on superexchange or tunnelling interactions [48]. Homobimetallic complexes of dppcb with Ru(II) also show these interactions, since preliminary experiments indicate that their photochemical behaviour is completely different from analogous compounds containing diphosphines.

Since $[Pd(CH_3CN)_4](BF_4)_2$ has been found to catalyse the polymerization of acetylenes and olefins [49], the complex $[Pd_2(dppcb)(DMF)_4](BF_4)_4$ presented above could show comparable catalytic properties. Furthermore, Pd(II) complexes of $PhP(CH_2CH_2PPh_2)_2$ catalyse the electrochemical reduction of CO_2 to CO [18,50]. In this paper it is shown that compounds of the type $[Pd_2(dppcb)(monophosphine)_4]^{4+}$ are possible. Therefore, also $[Pd(dppcb)_2]^{2+}$ could be prepared. Similar to the chelating bis(phosphine) 3,5-bis[(diphenylphosphino)methyl]pyridine, which forms a trinuclear Pd complex, a metalloligand like $[Pd(dppcb)_2]^{2+}$ offers a straightforward approach for the generation of oligonuclear and multinuclear complexes [51]. Further work on this is in progress.

Supplementary data

Details on the structure determinations, atomic fractional coordinates and other relevant data are obtainable from the Cambridge Crystallographic Data Centre, 12 Union Road, Cambridge CB2 1EZ, UK on request (fax: +44-1223-336033; e-mail: deposit@ccdc.cam.ac.uk). The crystal structures of $[Pt_2I_4(trans\text{-}dppen)_2]$ (**1**), $[Pd_2Cl_4(dppcb)]$ (**3**), and *trans*-$[Pd_2Cl_2(dppcb)(PMePh_2)_2](BF_4)_2$ (**10**) have been allocated the deposition numbers CCDC 137542, CCDC 137543, and CCDC 137544, respectively.

Acknowledgements

We thank the Fonds zur Förderung der wissenschaftlichen Forschung, Austria, for financial support.

References

[1] H.C. Clark, G. Ferguson, P.N. Kapoor, M. Parvez, Inorg. Chem. 24 (1985) 3924.
[2] W. Oberhauser, C. Bachmann, T. Stampfl, P. Brüggeller, Inorg. Chim. Acta 256 (1997) 223.
[3] G. Hogarth, T. Norman, Polyhedron 15 (1996) 2859.
[4] J.M. Vila, M. Gayoso, M.T. Pereira, J.M. Ortigueira, A. Fernandez, N.A. Bailey, H. Adams, Polyhedron 12 (1993) 171.
[5] J.M. Vila, M. Gayoso, A. Fernandez, N.A. Bailey, H. Adams, J. Organomet. Chem. 448 (1993) 233.
[6] R.B. King, P.N. Kapoor, Inorg. Chem. 11 (1972) 1524.
[7] W. Oberhauser, C. Bachmann, T. Stampfl, R. Haid, C. Langes, H. Kopacka, A. Rieder, P. Brüggeller, Inorg. Chim. Acta 290 (1999) 167.
[8] W. Oberhauser, C. Bachmann, T. Stampfl, R. Haid, C. Langes, A. Rieder, P. Brüggeller, Polyhedron 17 (1998) 3211.
[9] M.R. Mason, C.M. Duff, L.L. Miller, R.A. Jacobson, J.G. Verkade, Inorg. Chem. 31 (1992) 2746.
[10] E. Drent, P.H.M. Budzelaar, Chem. Rev. 96 (1996) 663.
[11] M. Formica, C. Carfagna, G. Gatti, A. Musco, 33rd Int. Conf. on Coordination Chemistry, Florence, Italy, August 30–September 4, 1998, Book of Abstracts, p. 470.
[12] M. Gómez, G. Muller, J. Sales, X. Solans, J. Chem. Soc., Dalton Trans. (1993) 221.
[13] A.C.T. North, D.C. Phillips, F.S. Mathews, Acta Crystallogr., Sect. A 24 (1968) 351.
[14] G.M. Sheldrick, Acta Crystallogr., Sect. A 46 (1990) 467.
[15] G.M. Sheldrick, SHELXL-97, a computer program for crystal structure determination, University of Göttingen, Germany, 1997.
[16] P.S. Pregosin, R.W. Kunz, in: P. Diehl, E. Fluck, R. Kosfeld (Eds.), NMR Basic Principles and Progress, vol. 16, Springer, Berlin, 1979, p. 16
[17] E.G. Hope, W. Levason, N.A. Powell, Inorg. Chim. Acta 115 (1986) 187.
[18] H.A. Mayer, W.C. Kaska, Chem. Rev. 94 (1994) 1239.
[19] A. Martin, A.G. Orpen, J. Am. Chem. Soc. 118 (1996) 1464.
[20] H.-L. Ji, J.H. Nelson, A. DeCian, J. Fischer, C. Li, C. Wang, B. McCarty, Y. Aoki, J.W. Kenny III, L. Solvjic, E.B. Milosavljevic, J. Organomet. Chem. 529 (1997) 395.
[21] R. Gilardi, C. George, J.L. Flippen-Anderson, Acta Crystallogr., Sect. C 48 (1992) 1680.
[22] J.A. Rahn, D.J. O'Donnell, A.R. Palmer, J.H. Nelson, Inorg. Chem. 28 (1989) 2631.
[23] W. Oberhauser, C. Bachmann, P. Brüggeller, Polyhedron 14 (1995) 787.
[24] W.L. Steffen, G.L. Palenik, Inorg. Chem. 15 (1976) 2432.
[25] A.J. Paviglianiti, D.J. Minn, W.C. Fultz, J.L. Burmeister, Inorg. Chim. Acta 159 (1989) 65.
[26] S. Singh, N.K. Jha, P. Narula, T.P. Singh, Acta Crystallogr., Sect. C 51 (1995) 593.
[27] L.R. Gray, D.J. Gulliver, W. Levason, M. Webster, Inorg. Chem. 22 (1983) 2362.
[28] S.E. Saum, S.A. Laneman, G.G. Stanley, Inorg. Chem. 29 (1990) 5065.
[29] F.P. Fanizzi, G. Natile, M. Lanfranchi, A. Tiripicchio, F. Laschi, P. Zanello, Inorg. Chem. 35 (1996) 3173.
[30] P.E. Garrou, Chem. Rev. 81 (1981) 229.
[31] B. Bendiksen, W.C. Riley, M.W. Babich, J.H. Nelson, R.A. Jacobson, Inorg. Chim. Acta 57 (1982) 29.
[32] W. Oberhauser, C. Bachmann, P. Brüggeller, Inorg. Chim. Acta 238 (1995) 35.
[33] P. Brüggeller, Z. Naturforsch., Teil B 41 (1986) 1561.
[34] A.L. Balch, B.J. Davis, E.Y. Fung, M.M. Olmstead, Inorg. Chim. Acta 212 (1993) 149.
[35] P. Ghosh, A. Chakravorty, Inorg. Chem. 36 (1997) 64.
[36] K. Nakamoto, Infrared and Raman Spectra of Inorganic and Coordination Compounds, Wiley, New York, 5th edn., 1997, Part B, p. 49.
[37] C. Bachmann, C. Langes, T. Stampfl, R. Haid, H. Kopacka, K.-H. Ongania, P. Brüggeller, to be published.
[38] A. Castiñeiras, E. Bermejo, D.X. West, L.J. Ackerman, J. Valdés-Martínez, S. Hernández-Ortega, Polyhedron 18 (1999) 1463.
[39] M. Mizutani, I. Kubo, K. Jitsukawa, H. Masuda, H. Einaga, Inorg. Chem. 38 (1999) 420.
[40] R. Giannandrea, P. Mastrorilli, C.F. Nobile, Inorg. Chim. Acta 284 (1999) 116.
[41] S.E. Saum, G.G. Stanley, Polyhedron 6 (1987) 1803.

[42] K.D. Tau, D.W. Meek, Inorg. Chem. 18 (1979) 3574.
[43] G. Dyer, J. Roscoe, Inorg. Chem. 35 (1996) 4098.
[44] C. Bianchini, H.M. Lee, A. Meli, W. Oberhauser, F. Vizza, P. Brüggeller, R. Haid, C. Langes, to be published.
[45] C. Bianchini, A. Meli, M. Peruzzini, F. Vizza, F. Zanobini, Coord. Chem. Rev. 120 (1992) 193.
[46] F.A. Cotton, B. Hong, Prog. Inorg. Chem. 40 (1992) 179.
[47] D.G. McCollum, G.P.A. Yap, A.L. Rheingold, B. Bosnich, J. Am. Chem. Soc. 118 (1996) 1365.
[48] P.-W. Wang, M.A. Fox, Inorg. Chem. 34 (1995) 36.
[49] A. Sen, T.-W. Lai, Organometallics 1 (1982) 415.
[50] D.L. DuBois, A. Miedaner, J. Am. Chem. Soc. 109 (1987) 113.
[51] A. Weisman, M. Gozin, H.-B. Kraatz, D. Milstein, Inorg. Chem. 35 (1996) 1792.